2D1-3

Asymptotic Analysis Methods for Scattered Fields by a Coated Conducting Cylinder

[#] Le Hoang Loc and Keiji Goto
Department of Communication Engineering, National Defense Academy
Yokosuka, Kanagawa, Japan, keigoto@nda.ac.jp

1. Introduction

The problems of the High-frequency (HF) scattering by coated conducting cylinder covered by a dielectric material have been an important research subject in the area of radar cross section, antennas and propagation, and so on [1], [2].

We have derived in [3] the extended uniform geometrical theory of diffraction (extended UTD) solution for the scattered fields by a coated conducting cylinder with a lossy medium. The extended UTD solution characterized by an impedance boundary condition (IBC) and effective in the transition region near the shadow boundary (SB) in [3] has agreed excellently with the exact solution when the thickness of coating medium is thin. However, the accuracy of the asymptotic solution in [3] deteriorates gradually as the thickness of coating medium becomes thick. In order to solve the above problem, it is necessary to newly take existance of the p th times reflected geometrical boundary (GB_p) into consideration where the GB_p denotes the tangent line at the refraction point of a coating surface after reflected p times on a conducting cylinder (see Fig.2).

In this paper, we study the asymptotic analysis methods taken into account the effect of the scattering phenomena inside a coating medium. Specifically, we derive both an extended UTD solution for a reflected-surface diffracted ray (RSD) effective in the transition region near the GB_p and a reflected-geometrical ray (RGO) solution in the lit region away from the GB_p. The validity and the applicability of the asymptotic solutions derived here are confirmed by comparing with the exact solution obtained from the eigenfunction expansion [3], [4].

2. Formulation and Integral Representation for Scattered Fields

Figure 1 shows a surrounding medium 1 (ε_1, μ_0) and a coated conducting cylinder of radius a covered by a complex dielectric medium 2 (ε_2^*, μ_0) of thickness $t\,(=a-b)$, and coordinate systems (x,y,z) and (ρ,ϕ,z). We examine the two-dimensional problem assuming that the electric line source $\mathrm{Q}(\boldsymbol{\rho}')$, $\boldsymbol{\rho}'=(\rho',\phi')$ is placed parallel to the coated cylinder.

The integral representation for the scattered fields E_z^s observed at a point $\mathrm{P}(\boldsymbol{\rho})$, $\boldsymbol{\rho}=(\rho,\phi)$, may be given by the following summation of the three kinds of integrals [4]:

$$E_z^s = E_{z,1} + E_{z,2} + E_{z,3} \tag{1}$$

Here, $E_{z,1}$ denotes the integral representing the direct ray before passing through a turning point (TP) and $E_{z,2}$ is the integral including both the direct ray after passing through a TP and the scattering phenomena on the coating surface. While, $E_{z,3}$ denotes the integral including the scattering phenomena inside the coating medium 2 and may be represented as follows:

$$E_{z,3} = \sum_{p=1}^{\infty} E_{z,3}^p \tag{2}$$

$$E_{z,3}^p = \frac{i}{8}\int_{-\infty}^{\infty} \kappa_1 T_{12} T_{21} (\kappa_2^p R_{22}^{p-1})\, H_v^{(1)}(k_1\rho') H_v^{(1)}(k_1\rho) \exp(iv|\phi-\phi'|)\mathrm{d}v \tag{3}$$

$$\kappa_1 = -\frac{H_v^{(2)}(k_1 a)}{H_v^{(1)}(k_1 a)}, \quad \kappa_2 = -\frac{H_v^{(1)}(k_2^* a) H_v^{(2)}(k_2^* b)}{H_v^{(2)}(k_2^* a) H_v^{(1)}(k_2^* b)} \tag{4}$$

$$T_{12} = 1 + R_{11}\,,\ T_{21} = 1 + R_{22} \tag{5}$$

$$R_{11} = -\frac{\log' H_v^{(2)}(k_2^* a) - Z_s \log' H_v^{(2)}(k_1 a)}{\log' H_v^{(2)}(k_2^* a) - Z_s \log' H_v^{(1)}(k_1 a)}\,,\quad R_{22} = -\frac{\log' H_v^{(1)}(k_2^* a) - Z_s \log' H_v^{(1)}(k_1 a)}{\log' H_v^{(2)}(k_2^* a) - Z_s \log' H_v^{(1)}(k_1 a)} \tag{6}$$

Here $H_v^{(1)}(\cdot)$ and $H_v^{(2)}(\cdot)$ denote the Hankel functions of the first and the second kinds [5], respectively, and the prime ($'$) on the functions denotes the derivative with respect to the argument. $k_1 = \omega(\varepsilon_1\mu_0)^{1/2}$ ($k_2^* = \omega(\varepsilon_2^*\mu_0)^{1/2}$) and $Z_1 = (\mu_0/\varepsilon_1)^{1/2}$ ($Z_2 = (\mu_0/\varepsilon_2^*)^{1/2}$) are the wavenumber and the characteristic impedance of the medium 1 (the medium 2). Notation ε_2^* denotes the complex dielectric constant of the material 2 and is defined by $\varepsilon_2^* = \varepsilon_2 + i\sigma_2/\omega$ where σ_2 is the conductivity. Notation $p(= 1, 2, \cdots)$ in (2) and (3) denotes the number of reflection on the conducting cylinder $\rho = b$. The time convention $\exp(-i\omega t)$ is adopted and suppressed here.

3. Asymptotic Solutions Including Scattering Phenomena inside Coating Medium

Figure 2 shows the shadow boundary SB ($= \mathrm{GB}_{p=0}$) and the once ($p = 1$) reflected geometrical boundary $\mathrm{GB}_{p=1}$ (GB_1) where p denotes the number of reflection on the conducting cylinder ($\rho = b$). The surrounding medium 1 is divided into the lit and the shadow region by the GB_1. When the observation point is located in the lit region away from the GB_1, the once reflected-geometrical ray ($\mathrm{RGO}_{p=1}$) (RGO_1) is observed. While, we observe the once reflected-surface diffracted ray ($\mathrm{RSD}_{p=1}$) (RSD_1) when the observation point is located in the shadow region far away from the GB_1. In this section, we will derive the asymptotic solutions including the scattering phenomena inside a coating medium 2.

3.1 Extended UTD Solution for Reflected-Surface Diffracted Ray

In this section, from the integral $E_{z,3}^p$ in (3), we will derive the extended UTD solution for the p th reflected-surface diffracted ray (RSD_p) applicable uniformly in the transition region near the GB_p and in the deep shadow region far away from the GB_p.

In the shadow region, the main contribution to the integral $E_{z,3}^p$ in (3) arises from the portion of the integration path near $v = k_1 a$ in the complex v-plane. In this case, one may replace the functions $H_v^{(1),(2)}(k_1 a)$ and $H_v^{(1),(2)\prime}(k_1 a)$ by their Airy approximations [5] and the function $H_v^{(1)}(k_1 x), x = \rho'$ or $x = \rho$, by the Debye's approximation [5], respectively, with the transformation from the complex v-plane to the complex τ-plane via $v = k_1 a + M\tau,\ M = (k_1 a/2)^{1/3}$. Then by performing the straightforward manipulation, one may obtain the following extended UTD solution [4].

$$E_{z,3}^p \sim G(k_1 L_1)\exp(ik_2^* L_t + ik_1 \ell)(R_2)^p I(\xi) G(k_1 L_2) \tag{7}$$

$$G(k_1 L_{1,2}) = \frac{i}{4}\sqrt{\frac{2}{\pi k_1 L_{1,2}}}\exp(ik_1 L_{1,2} - i\pi/4) \tag{8}$$

$$I(\xi) = \frac{i8M^2}{\pi Z_s}\cos\theta_c \int_{C_\tau} \exp\left[\left\{i\xi\tau + i\left(\frac{M^2}{2k_1 L_1} + \frac{M^2}{2k_1 L_2} + \frac{(2p)M^2}{2k_2^* a\cos\theta_c} - \frac{(2p)M^2}{2k_2^* b\cos\theta_i}\right)\tau^2\right\}\right.$$
$$\left.\cdot\frac{\{-(w_1'(\tau) + q(\tau)w_1(\tau))\}^{p-1}}{(w_1'(\tau) - q(\tau)w_1(\tau))^{p+1}}\right] d\tau\,,\quad q(\tau) = iM\frac{\sqrt{(k_2^* a)^2 - v^2}}{k_2^* a}\frac{1}{Z_s} \tag{9}$$

$$M = (k_1 a/2)^{1/3}\,,\ R_2 = -1\,,\ \xi = M\{\theta - (2p)\psi\},\ Z_s = Z_2/Z_1, \tag{10}$$

$$\theta = |\phi - \phi'| - \cos^{-1}(a/\rho') - \cos^{-1}(a/\rho),\quad \psi = \cos^{-1}(k_1/k_2^*) - \cos^{-1}(k_1 a/k_2^* \mathrm{b}) \tag{11}$$

$$L_1 = \sqrt{\rho'^2 - a^2},\ L_2 = \sqrt{\rho^2 - a^2},\ \ell = a(\theta - (2p)\psi),\ L_t = (2p)(a\cos\theta_c - b\cos\theta_i) \tag{12}$$

where notations $w_s(= \pi/2)$ and θ_c denote respectively the incident angle and the refraction angle on the surface $\rho = a$, and θ_i is the incident angle to the conducting cylinder $\rho = b$ (see Fig.2).

We have also shown in Fig.2 the propagation path of the once reflected-surface diffracted ray $E_{z,3}^1$ with $p = 1$ in (7)-(12). Notations L_1, L_t, ℓ and L_2 may be interpreted as follows. $L_1(= \mathrm{Q} \rightarrow$

Q_1) denotes the propagation distance (path) of the incident cylindrical wave which illuminates the surface diffraction point Q_1 from the source point Q, $L_t(= Q_1 \to Q_2 \to Q_3)$ denotes the propagation distance (path), where Q_2 denotes the reflection point on the conducting cylinder $\rho = b$, passing through the medium 2, $\ell(= Q_3 \curvearrowright Q_4)$ the propagation distance (path) of the creeping wave along on the convex surface $\rho = a$, and $L_2(Q_4 \to P_2)$ the propagation distance (path) from the diffraction point Q_4 to the observation point P_2. Notation $G(k_1 L_{1,2})$ in (8) is the 2-dimensional free space Green's function and the integral $I(\xi)$ in (9) may be interpreted as the term including the effect of scattering phenomena that occurs on the propagation path from the point Q_1 to the point Q_4.

3.2 Reflected-Geometrical Ray Solution

In this section, from the integral $E_{z,3}^p$ in (3), we will derive in the p th reflected-geometrical ray (RGO_p) solution applicable in the deep lit region far away from the GB_p.

In the deep lit region, the main contribution to the integral $E_{z,3}^p$ in (3) arises from the portion of the integration path near $v = k_1 a$ in the complex v -plane. One may replace all the Hankel functions in (3) by the Debye's approximation [5] with the transformation from the complex v -plane to the complex w -plane via $v = k_1 a \sin w$. Then by applying the saddle point technique [6], one may obtain the p th reflected-geometrical ray (RGO_p) solution [4]. The reader may be obtain the explicit RGO_p solution in [4].

4. Numerical Results and Discussions

In order to confirm the validity and the applicability of the asymptotic solutions derived in Section **3**, we have calculated the scattered fields by a coated conducting cylinder illuminated by the incident electric-type cylindrical wave.

Figure 3 shows the scattered field strength vs. $|\phi - \phi'|$ curves. The shadow boundary SB ($= GB_0$) is located at $|\phi - \phi'| = 95.7°$, and the region in which the p th reflected-surface diffracted ray RSD_p can be observed is shown by the notation ◄—, in the figure. The asymptotic solution (○○○: open circles) is obtained by using the direct ray, the reflected ray on the surface $\rho = a$, and up to 3 times reflected-geometrical ray $RGO_{p=3}$ on the conducting cylinder $\rho = b$. The asymptotic solution (●●●: closed circles) is obtained by using both the extended UTD solution for the surface diffracted ray ($p = 0$) along the surface $\rho = a$ and the extended UTD solution series for the RSD_p in (2). It is observed that the asymptotic solutions (○○○ and ●●●) agree excellently with the exact solution (——: solid curve) in each region.

Also shown in Fig.3 is the conventional GO solution [3] (the direct ray and the reflected ray on the surface $\rho = a$) (----: dashed curve) for the lit region and the conventional extended UTD solution [3] (---- : dashed curve) for the region ($46.0° \leq |\phi - \phi'| \leq 180.0°$). The conventional GO solution agrees well in the lit region. However, the conventional extended UTD solution becomes inaccurate in the region ($46.0° \leq |\phi - \phi'| \leq 180.0°$). It is clarified that the conventional extended UTD solution produces the large errors in the transition and the shadow region.

5. Conclusion

We have derived the extended UTD solution for the reflected-surface diffracted ray and the reflected-geometrical ray solution taken into account the effect of the scattering phenomena inside the coating medium of a coated conducting cylinder. The accuracy of the asymptotic solutions derived here has been confirmed by comparing with the exact solution.

Acknowledgments

This work was supported in part by the Grant-in-Aid for Scientific Research (C) (24560492) from Japan Society for the Promotion of Science (JSPS).

References

[1] H. T. Kim and N. Wang, “UTD solution for electromagnetic scattering by a circular cylinder with thin loss coatings”, IEEE Trans. Antennas Propagat., vol. 37, no. 11, pp. 1463-1472, Nov. 1989.

[2] P. E. Hussar, “A uniform GTD treatment of surface diffraction by impedance and coated cylinders”, IEEE Trans. Antennas Propagat., vol. 46, no. 7, pp. 998-1008, July 1998.

[3] K. Goto, L. H. Loc, T. Kawano, and T. Ishihara, “Asymptotic analysis of high-frequency scattered fields by a coated conducting cylinder” (in Japanese), The Papers of Technical Meeting on EMT, IEE Japan, EMT-11-128, pp. 1-6, Nov. 2011.

[4] L. H. Loc, K. Goto, T. Kawano, and T. Ishihara, “Extended UTD solution for high-frequency scattered fields by a coated conducting cylinder” (in Japanese), The Papers of Technical Meeting on EMT, IEE Japan, EMT-12-18, pp. 73-78, Jan. 2012.

[5] M. Abramowitz and I. A. Stegun, *Handbook of Mathematical Functions*, Dover, New York, pp.358-478, 1972.

[6] L. B. Felsen and N. Marcuvitz, *Radiation and Scattering of Waves*, Chaps. 4 and 5, IEEE Press, New Jersey, 1994.

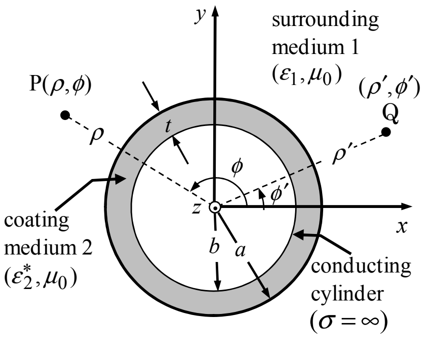

Fig.1 Coated conducting cylinder, and coordinate systems (x, y, z) and (ρ, ϕ). Q: electric line source, P: observation point.

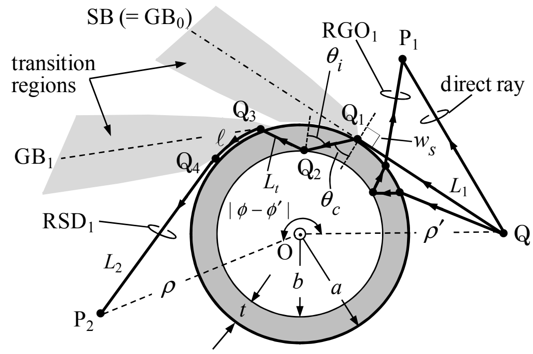

Fig.2 Direct ray, once reflected-geometrical ray RGO_1, and once reflected-surface diffracted ray RSD_1. Also shown are the transition regions near the SB $(= GB_0)$ and GB_1.

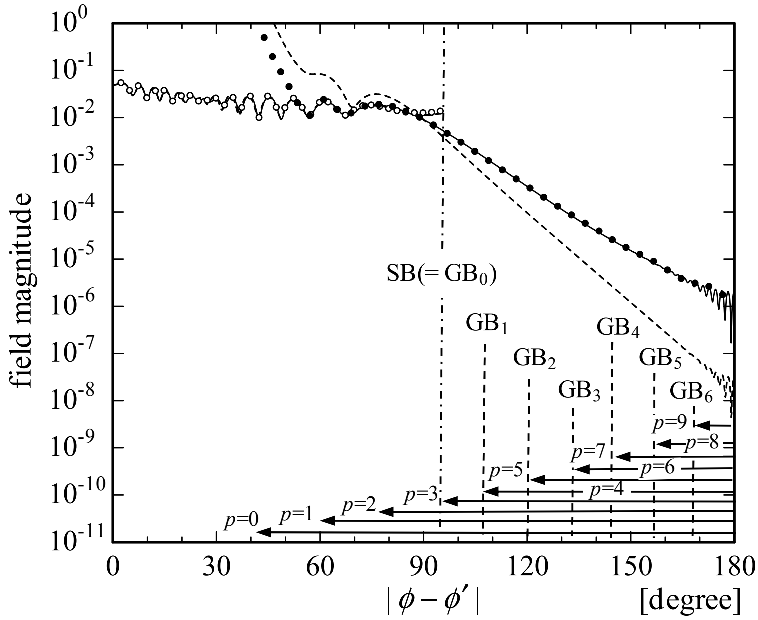

Fig.3 Scattered fields by a coated conducting cylinder calculated from the asymptotic solutions and exact solution. The numerical parameters used in the calculation: $a = 5.0$, $k_1 a = 100, t = 2.0\lambda$, $\varepsilon_1 = \varepsilon_0$, $\varepsilon_2^* = \varepsilon_0 \varepsilon_{2r}$, $\varepsilon_{2r} = 3 + i0.1$, source point: $(\rho', \phi') = (7.0, 0.0°)$ and observation point: $(\rho, \phi) = (8.0, \phi)$. ∘∘∘ : asymptotic solution including RGO_p, ●●● : asymptotic solution including RSD_p, —— : exact solution, - - - -: conventional asymptotic solutions.